第 35 卷第 1 期 无 机 化 学 学 报 Vol.35 No.1
2019 年 1 月 CHINESE JOURNAL OF INORGANIC CHEMISTRY 116-124

片状纳米结构 CeO_2 晶体的制备及其吸附 CO_2 性能

赵博生[1,2] 史会虎[1,2] 马 良[1,2] 杜 宏[1,2] 张建斌*,[1,2]
([1] 内蒙古工业大学化工学院,呼和浩特 010051)
([2] 内蒙古自治区 CO_2 捕集与资源化工程研究中心,呼和浩特 010051)

摘要: 在室温下,将 $CeCl_3$ 溶液与 CO_2 储存材料(CO_2SM)混合、搅拌 0.5 h 制备了片状碳酸铈前驱体(CCPs),并在 500 ℃下煅烧 CCPs 4 h,制得平均尺寸为 4.94 μm×0.92 μm,厚度为 0.04~0.08 μm 纳米结构片状 CeO_2 晶体。在此过程中,CO_2SM 不但可以提供 CO_3^{2-},还能起到分散剂和结构导向剂的作用。反应过程中,系统地研究了 CO_2SM 用量、Ce^{3+}浓度和搅拌时间 3 个因素对 CCPs 形态和大小的影响, 得到最优制备条件:0.1 g CO_2SM 和 50 mL 0.03 mol·L^{-1} Ce^{3+}水溶液以 1 000 r·min^{-1} 转速在室温下搅拌 0.5 h。煅烧 CCPs 后,所制备的片状 CeO_2 晶体在室温下 CO_2 吸附量可达 0.554 mmol·g^{-1}。

关键词: CeO_2 晶体; 碳酸铈前体; CO_2 储存材料; CO_2 吸附
中图分类号: O611 **文献标识码**: A **文章编号**: 1001-4861(2019)01-0116-09
DOI:10.11862/CJIC.2019.019

Preparation and CO_2 Adsorption Property of Flake-like Nano-Structure CeO_2 Crystals

ZHAO Bo-Sheng[1,2] SHI Hui-Hu[1,2] MA Liang[1,2] DU Hong[1,2] ZHANG Jian-Bin*,[1,2]
([1]*College of Chemical Engineering, Inner Mongolia University of Technology, Hohhot* 010051, *China*)
([2]*Inner Mongolia Engineering Research Center for CO_2 Capture and Utilization, Hohhot* 010051, *China*)

Abstract: Nano-structure flake-like CeO_2 crystals with an average size of 4.94 μm×0.92 μm (length and width) and the thickness of 0.04~0.08 μm were prepared by simply calcining cerium carbonate precursors (CCPs) at 500 ℃ for 4 h, in which the flake-like CCPs were firstly prepared by stirring $CeCl_3$ aqueous solution with CO_2-storage material (CO_2SM) for 0.5 h at room temperature. Interesting, the CO_2SM could provide CO_3^{2-} and act as dispersant and structure-directing agent for the preparation of flake-like CCPs. In the process, the effect of three factors, including CO_2SM dosage, Ce^{3+} concentration and stirring time, on the morphology and size of CCPs were systemically studied, and the optimum preparation conditions of flake-like CCPs were confirmed at 0.1 g CO_2SM with 50 mL 0.03 mol·L^{-1} Ce^{3+} aqueous solution at 1 000 r·min^{-1} for 0.5 h at room temperature. After calcining CCPs, the as-prepared flake-like CeO_2 crystals presented the CO_2 adsorption amount of 0.554 mmol·g^{-1} at room temperature.

Keywords: CeO_2 crystals; cerium carbonate precursors; CO_2-storage material; CO_2 adsorption

In the past years, steel plants, thermal power plants and chemical plants emitted large amounts of CO_2 gas every year, causing environmental pollution to become more serious, which had become the focus of global attention[1-3]. In general, amine solutions were often used to treat CO_2 in industrial exhaust gases[4].

收稿日期:2018-08-30。收修改稿日期:2018-11-26。
煤基 CO_2 捕集与封存国家重点实验室项目(No.2016A06)、国家自然科学基金(No.21666027)、内蒙古自治区“草原英才”、内蒙古杰出青年基金(No.2016JQ02)、内蒙科委攻关资助项目和内蒙古工业大学青年学术骨干培养项目资助。
*通信联系人。E-mail:tadzhang@pku.edu.cn

However, the amine solutions presented high volatile and corrosive, which increased the treatment cost of industrial exhaust gas[5]. To solve the shortcomings of the amine solutions, more stable and economical method for CO_2 capture should be developed. A new type of solid adsorbent had stable structure, chemical properties and efficient cycle performance, which could be used to capture CO_2 in industrial exhaust, such as metal oxides[6-10], carbon-materials[11-13], silica-materials[14-17], metal organic frameworks[18-20] and zeolites[21-23]. The main reason for studying metal oxides was that metal oxides had a higher true density than other materials[24]. Especially, CeO_2 materials could be used as the good solid CO_2 adsorbent due to its strong Lewis base sites[25-26]. Normally, CeO_2 crystals were prepared by calcining CCPs, which had been synthesized through many methods, such as hydrothermal methods[27-28], sol-gel methods[29-30], precipitation methods[31], solvothermal methods[32-33] and microwave methods[34-35]. However, these synthetic methods had a long reaction time and required additional template additive, resulting in high cost[36-38].

Based on the above discussion, this work proposed a simple synthesis method without additional additives for facile preparation of nano-structure flake-like CCPs, which mixed $CeCl_3$ solution with CO_2SM at room temperature and stirred at a certain rotational speed. The nano-structure flake-like CeO_2 crystals were obtained by calcining CCPs for 4 h at 500 ℃. In the synthesis process, the CO_2SM played a significant role, which provide CO_3^{2-} and act as dispersant and structure-directing agent. The effect of three factors on the morphology and size of flake-like CCPs were studied, including CO_2SM dosage, Ce^{3+} concentration and stirring time. The flake-like CeO_2 crystals not only had good reduction performance, but also could capture CO_2 and reached 0.554 mmol·g^{-1} at room temperature. Fig.1 shows the entire preparation process. CCPs prepared through stirring CO_2SM and Ce^{3+} and CeO_2 was obtained by calcining CCPs, which could adsorb CO_2. CO_2SM was synthesized by absorbing CO_2 with ethylene glycol (EG) and 1,2-ethanediamine (EDA).

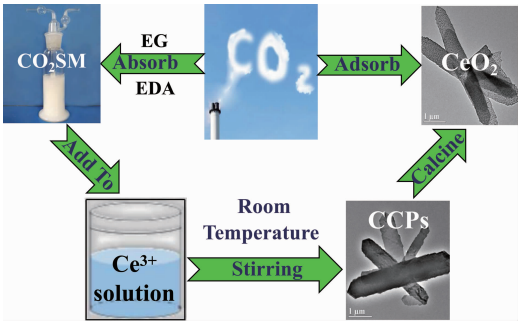

Fig.1　Entire preparation process

1　Experimental

1.1　Materials

EG and EDA was analytical grade. 99.999% (*V*/*V*) compressed CO_2 was obtained from the Standard Things Center. Cerium (Ⅲ) chloride heptahydrate ($CeCl_3 \cdot 7H_2O$) was purchased from Aladdin Company. The CO_2SM was synthesized by the EDA+EG system uptaking CO_2[39].

1.2　Preparation of CCPs and CeO_2 crystals

At room temperature, 0.1~0.5 g CO_2SM and 50 mL 0.01~0.1 mol·L^{-1} Ce^{3+} solution were mixed on the magnetic stirrer and stirred at 1 000 r·min^{-1} for 0.5~3 h to prepare CCPs. After the reaction, the CCPs were washed using double-distilled water and ethanol while being vacuum filtered and the precipitate was collected after repeated washing three times. To obtain the dried CCPs, the filtered precipitate was dried at 120 ℃ for 2 h. Finally, the nano-structure flake-like CeO_2 crystals were prepared by calcining CCPs at 500 ℃ with the heating step of 5 ℃·min^{-1} for 4 h in air.

1.3　Characterization

The CCPs and CeO_2 crystals were investigated by a Quanta FEG 650 scanning electron microscopy (SEM) with an accelerating voltage of 20 kV and a JEM-2100 high magnification transmission electron microscopy (HR-TEM) with an accelerating voltage of 200 kV. Their X-ray diffraction (XRD) patterns were collected on a Siemens D/max-RB powder X-ray diffract mete with Cu $K\alpha$ radiation (λ=0.154 059 8 nm) over the 2θ range of 10°~80° with the scanning rate of 0.05°·s^{-1} operated at 40 kV and 40 mA. Fourier transform infrared spectroscopy (FT-IR) was recorded on a Nexus 670 infrared spectrophotometer.

Isotherms were analyzed using 3H-2000PS2 BET instrument with the Barrett-Joyner-Halenda (BJH) theory to give the pore parameters, including Brunauer-Emmett-Teller (BET) surface area, total pore volume and average pore size. Entzsch-Sta 449 thermogravimetry analysis (TGA) was employed to measure the weight percentage of CCPs.

1.4 H_2 temperature-programmed reduction (H_2-TPR)

The H_2-TPR of CeO_2 crystals was measured through the TP-5080 equipment possessed a thermal conductivity detector (TCD). First, 50 mg CeO_2 crystals were placed in a quartz tube of the reactive furnace for heat treatment. The reactive furnace was heated to 400 ℃ through the temperature-programmed method for 30 min using N_2 as a shielding gas (30 mL·min^{-1}) to remove physically adsorbed H_2O and/or CO_2, and then cooled to room temperature. Then, hydrogen and nitrogen were mixed into a ratio of 5% (*V*/*V*) H_2, raising the temperature of the reactive furnace from room temperature to 1 000 ℃ with 10 ℃·min^{-1} to reduce CeO_2 crystals. Finally, the soft file of TP-5080 equipment was used to calculate the consumed amount of H_2 by CeO_2 crystals.

1.5 CO_2 temperature-programmed desorption (CO_2-TPD)

The alkalinity of CeO_2 crystals was measured by CO_2-TPD through the TP-5080 equipment possessed a TCD. First, 100 mg of CeO_2 crystals were placed in a quartz tube of a reaction furnace and heated at 400 ℃ for 30 min to perform heat treatment. Then, the pretreated CeO_2 crystals was adsorbed with pure CO_2 gas at room temperature, 120 and 700 ℃ for 30 min. After the adsorption, He gas was used to purge the CO_2 in the pipeline. The reaction furnace heated from room temperature to 1 000 ℃ with 10 ℃·min^{-1}. Finally, the soft file of TP-5080 equipment was used to calculate the amount of CO_2 consumed by CeO_2 crystals.

2 Results and discussion

2.1 Preparation of CCPs

In the experimental process, the influence of three factors of CO_2SM dosage, stirring time and Ce^{3+} ion concentration on the morphology and size of CCPs were systemically investigated.

2.1.1 CO_2SM dosages

To study the effect of CO_2SM dosage on the morphology and size of CCPs, the different amount of CO_2SM (0.1 ~0.5 g) was mixed with 50 mL water solution of 0.03 mol·L^{-1} Ce^{3+} using the magnetic stirrer. After stirring for 1 h at 1 000 r·min^{-1}, the CCPs were finally obtained. The size of CCPs were measured from SEM images.

According to the SEM images of CCPs in Fig.2, it could clearly observe the nano-structure flake-like CCPs. Through measuring the length and width of CCPs, it could be concluded that the size of the flake-

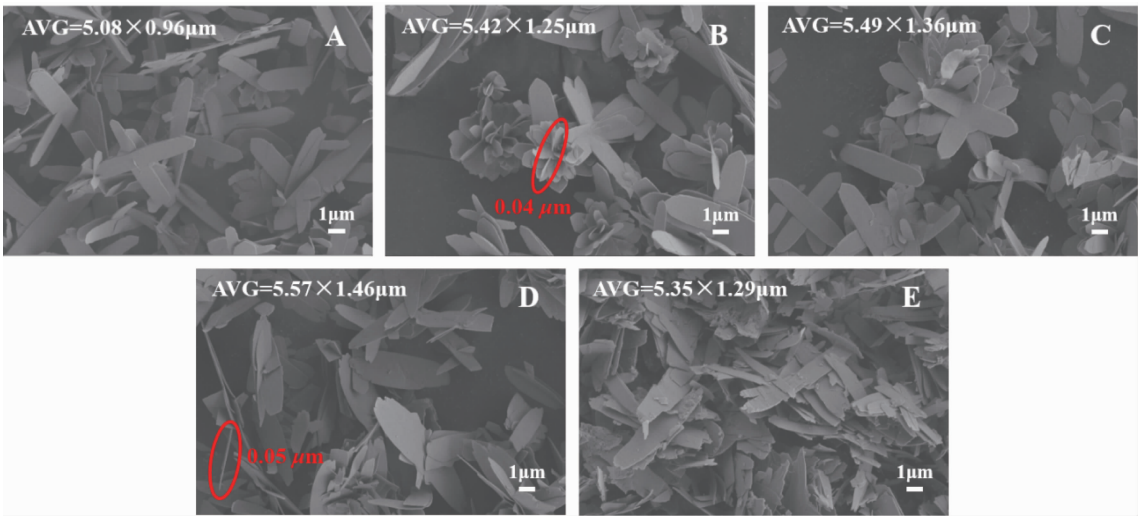

Fig.2 SEM images of CCPs under different CO_2SM dosages: (A) 0.1, (B) 0.2, (C) 0.3, (D) 0.4 and (E) 0.5 g

like CCPs gradually increased from 5.08 μm×0.96 μm in Fig.2A to 5.57 μm×1.46 μm in Fig.2D when the amount of CO_2SM increased from 0.1 to 0.4 g. When CO_2SM dosage continued to increase by 0.5 g, the size of flake-like CCPs reduced by 5.35 μm×1.29 μm, which was due to the formation of CCPs′ fracture. The 0.1 g CO_2SM could be used to prepare the minimum size of 5.08 μm×0.96 μm flake-like CCPs with the homogeneous morphology. Therefore, 0.1 g CO_2SM was selected for next experiment. Analysis of the effects of CO_2SM dosages on the morphology and size of CCPs, the more CO_2SM was dissolved in the solution, the more CO_3^{2-} would be generated and high nucleation rate of crystals. Therefore, as the CO_2SM dosages increased, the average diameter could gradually increase. However, when the CO_2SM dosages was too much, the morphology of CCPs would be broken to make the size smaller.

2.1.2　Ce^{3+} concentration

To study the effect of Ce^{3+} concentration on the morphology and size of CCPs, the 50 mL different concentrations of Ce^{3+} aqueous solution (0.01~0.1 mol·L^{-1}) was mixed with 0.1 g CO_2SM using the magnetic stirrer. After stirring for 1 h at 1 000 r·min^{-1}, the CCPs were finally obtained. The size of CCPs were measured from SEM images.

According to the SEM images of CCPs in Fig.3, it could be clearly observed that the Ce^{3+} concentrations did not affect the morphology of CCPs. When the Ce^{3+} concentration was 0.01 mol·L^{-1}, it could be seen that some small fragment CCPs were not uniform enough and the reunion phenomenon was serious. When the Ce^{3+} concentration increased from 0.03~0.1 mol·L^{-1}, the size of flake-like CCPs increased gradually from 5.08 μm×0.96 μm in Fig.3B to 5.89μm×1.22 μm in Fig. 3E. At the Ce^{3+} concentration of 0.03 mol·L^{-1}, the minimum size of flake-like CCPs with the homogeneous morphology could be obtained. Therefore, 0.03 mol·L^{-1} Ce^{3+} aqueous solution was used for next experiment. Analysis of the effects of Ce^{3+} concentration on the morphology and size of CCPs, the higher Ce^{3+} concentration, the higher the content of Ce^{3+} would generate more CCPs aggregates. Therefore, the size of the formed CCPs would become larger. Ce^{3+} concentration did not change the morphology of CCPs.

2.1.3　Stirring time

To study the effect of stirring time on the morphology and size of CCPs, the 50 mL 0.03 mol·L^{-1} Ce^{3+} aqueous solution was mixed with 0.1 g CO_2SM at different stirring times (0.5~3 h) using the magnetic stirrer. After stirring at 1 000 r·min^{-1}, the CCPs were finally obtained. The size of the CCPs were measured from SEM images.

According to the SEM images of CCPs in Fig.4, it could be clearly observed that the stirring time also did not affect the morphology of flake-like CCPs. By

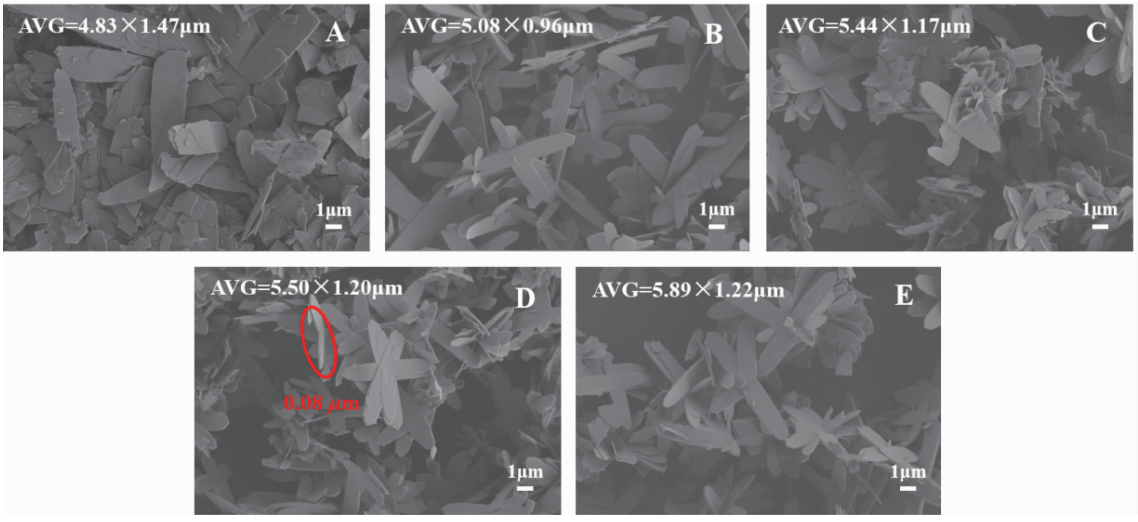

Fig.3　SEM images of CCPs under 50 mL different concentrations of Ce^{3+} aqueous solution: (A) 0.01, (B) 0.03, (C) 0.05, (D) 0.08 and (E) 0.1 mol·L^{-1}

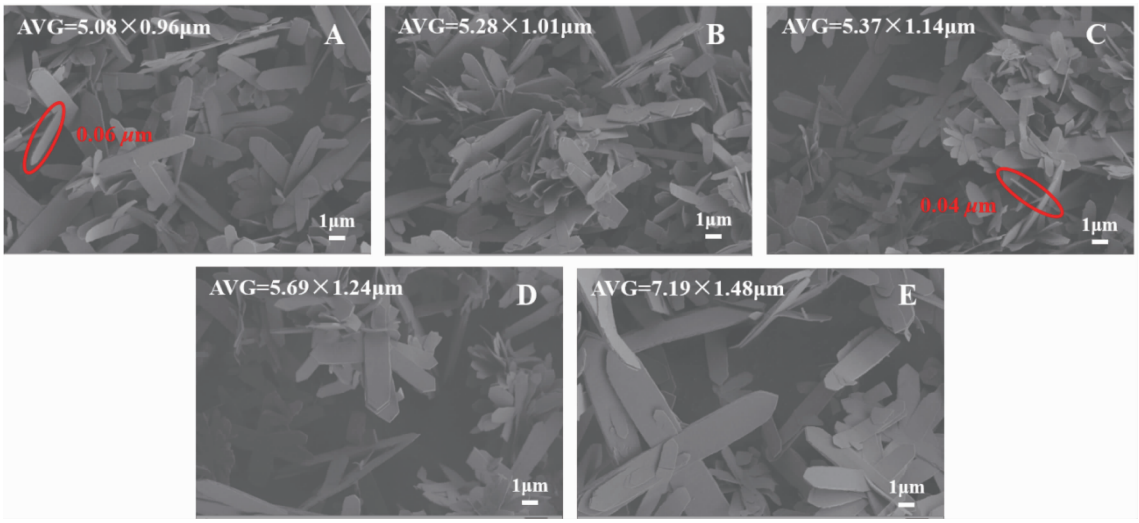

Fig.4 SEM images of CCPs under different stirring times: (A) 0.5, (B) 0.75, (C) 1, (D) 2 and (E) 3 h

measuring the size of the flake-like CCPs prepared at different stirring time, it could be concluded that the size of the flake-like CCPs increased gradually from the value of 5.08 μm×0.96 μm in Fig.4A to 7.19 μm×1.48 μm in Fig.4E with the increase of stirring time. The minimum size of the flake-like CCPs could be prepared at 0.5 h. Therefore, 0.5 h was chosen as the optimum stirring time. Analysis of the effects of stirring time on the morphology and size of CCPs, as time increased, the resulting CCPs aggregates also increased. Therefore, the size of the formed CCPs would become larger. Stirring time did not change the morphology of CCPs.

According to the XRD patterns of the CCPs in Fig.5(a), it could be observed that almost no diffraction peaks appeared in XRD patterns, indicating the prepared CCPs were amorphous. According to FT-IR spectrum of CCPs in Fig.5(b), it could be observed that the FTIR peak at 3 430 cm^{-1} occurred due to the O-H stretching vibration of -OH group and the peak shape had not changed with the time increasing[40-41]. The FT-IR absorption peak at 1 490 cm^{-1} was due to the double asymmetrical tensile vibration of the CO_3^{2-} group and the peak shape changed from package peak to sharp peak with the time increasing[42-43]. The other FT-IR peaks at 691, 754 and 843 cm^{-1} were due to bending vibration of the CO_3^{2-} group[44-45]. Analysis of FT-IR spectra showed that CCPs contained -OH and CO_3^{2-} groups.

Through the above three factors, the optimum preparation conditions were confirmed at 0.1 g CO_2SM with 50 mL 0.03 mol·L^{-1} Ce^{3+} aqueous solution at

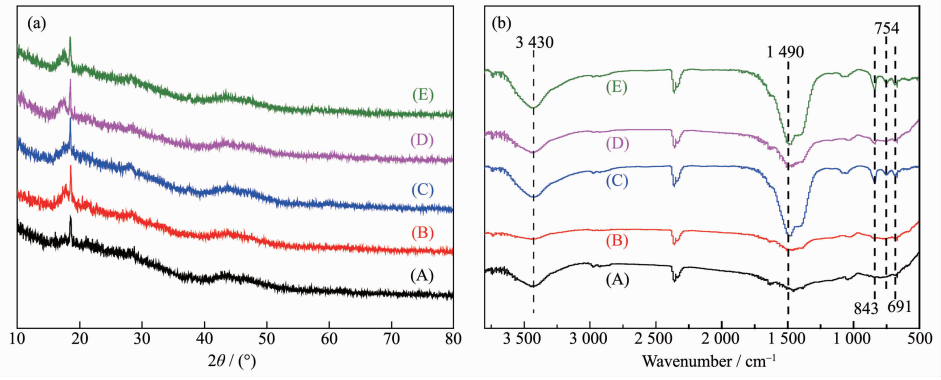

Other reaction conditions were as follows: 0.1 g CO_2SM, 50 mL 0.03 mol·L^{-1} Ce^{3+} water solution, room temperature and 1 000 r·min^{-1}

Fig.5 (a) XRD patterns and (b) FT-IR spectra of CCPs obtained after different stirring times: (A) 0.5, (B) 0.75, (C) 1, (D) 2 and (E) 3 h

1 000 r·min^{-1} for 0.5 h at room temperature.

2.2 Possible formation mechanism of CCPs

Fig.6 showed the possible formation mechanism of nano-structure flake-like CCPs, in which the CO_2SM played a crucial role in crystal nucleation and growth. The CO_2SM not only provided a source of CO_3^{2-} but also decomposed EG+EDA in aqueous solution[46]. Ce^{3+} was surrounded by EG/EDA because of the strong electrostatic interaction between EDA and EG[47]. This hindered the collision between Ce^{3+} and CO_3^{2-}, and eventually formed small CCPs aggregates. Small CCPs aggregates accumulated into the flake-like subunit structure due to hydrogen bonding between EDA and EG molecules. Moreover, the CO_2SM could also act as a dispersant and structure-directing agent[48]. Finally, the flake-like subunit structure could be freely assembled into flake-like CCPs.

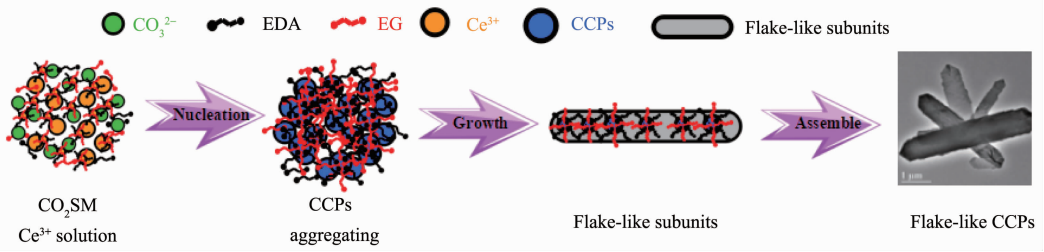

Fig.6　Possible formation mechanism of CCPs

2.3 TG-DTG

According to the typical TG-DTG curves of as-prepared CCPs in Fig.7, it could be found two distinct weight loss stages and the decomposition process of CCPs. The weight loss of the first stage occurred in the range of 50~314 ℃ and the weight loss of 5.51% was due to the evaporation of water and/or organic compounds that were physically or chemically absorbed on the surface of CCPs. The weight loss of the second stage occurred in the range of 314~684 ℃ and the large weight loss of 23.54% was due to the thermal decomposition of CCPs released CO_2. According to the DTG curve, it could be observed that the thermal decomposition of CCPs to CeO_2 was the endothermic process and the maximum endothermic peak occurred at 509 ℃. According to the TG-DTG curves, CeO_2 crystals were prepared by calcining CCPs at 500 ℃ for 4 h.

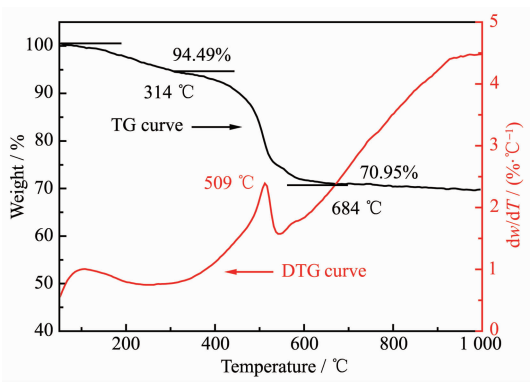

Fig.7　TG-DTG curves of as-prepared CCPs

2.4 XRD, SEM and TEM

XRD patterns of CeO_2 crystals were performed to determine the crystal form. According to the XRD patterns, the diffraction peaks at 2θ=28.560°, 33.160°, 47.550°, 56.480°, 59.291°, 69.510° and 76.780° corresponded to (111), (200), (220), (311), (222), (400) and (331) planes of face-centered cubic (FCC) CeO_2 crystals (PDF No.43-1002)[49].

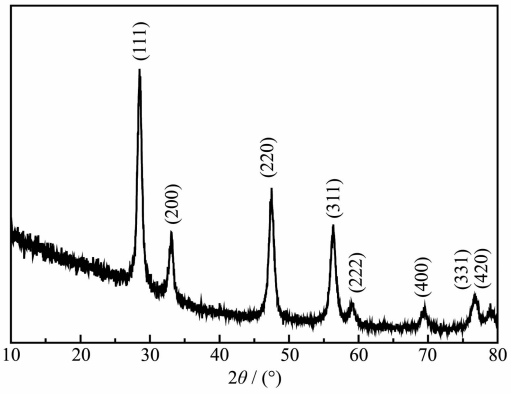

Fig.8　XRD patterns of flake-like CeO_2 crystals

Fig.9 was the SEM image of flake-like CeO_2 crystals. By comparing SEM images before and after calcining, it could be concluded that the calcination of CCPs at 500 ℃ did not change the original

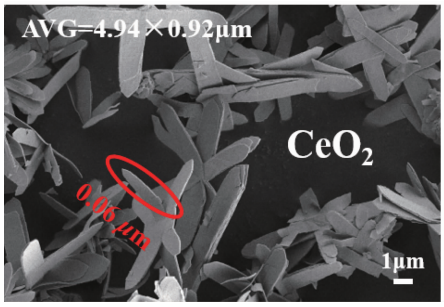

Fig.9 SEM image of flake-like CeO_2 crystals

morphology but only decreased in size from 5.08 μm× 0.96 μm to 4.94 μm ×0.92 μm. The thickness of flake-like CeO_2 crystals were measured at 0.06 μm.

From Fig.10A, the size of CCPs was 4.66 μm× 0.86 μm. The lattice spacing of CCPs were not clear and the crystal planes were complicated. The selected area electron diffraction (SAED) patterns of CCPs were composed of several bright rings, indicated that CCPs were amorphous. From Fig.10B, there were two flake-like CeO_2 crystals with dimensions of 4.93 μm× 0.64 and 4.91 μm ×0.67 μm. The flake-like CeO_2 crystals prepared after calcining became more transparent and the lattice spacing was clear. By measuring the distance between the black stripes, it could be concluded that the lattice spacing of 0.31 and 0.19 nm were equivalent to the (111) and (220) planes of the face-centered cubic CeO_2 crystals, respectively [50]. According to the SAED patterns, the distance from the bright spot to the center was measured to be 0.313 and 0.190 nm corresponding to the (111) and (220) planes of CeO_2 crystals, respectively. Therefore, it was shown that the flake-like CeO_2 crystals had a typical poly-crystalline structure.

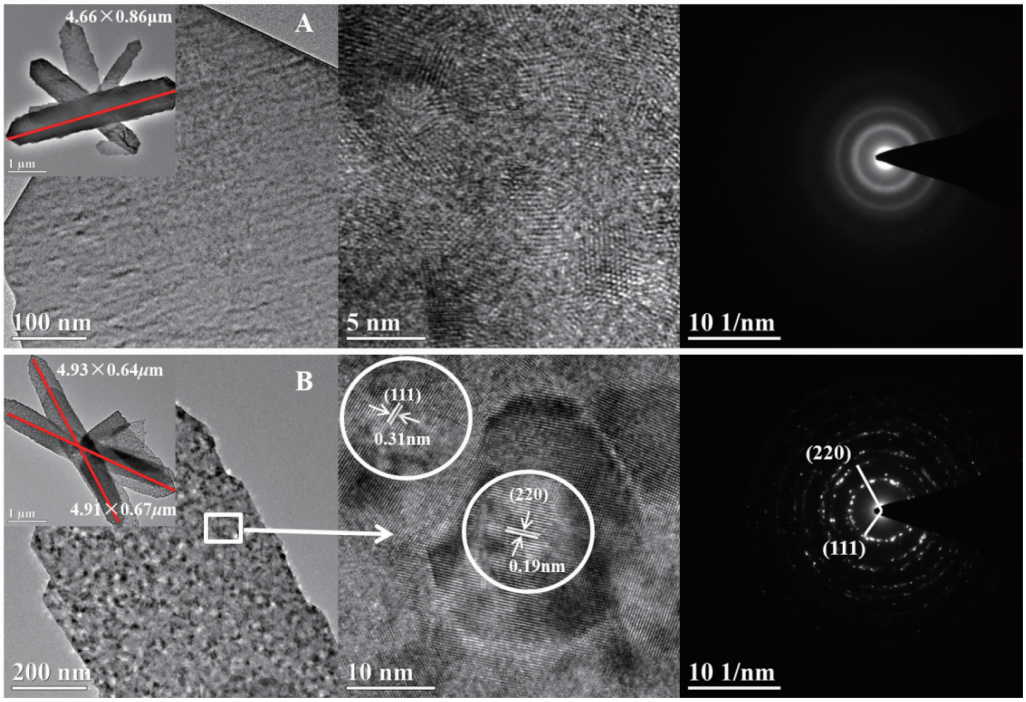

Fig.10 TEM images of CCPs (A) and CeO_2 crystals (B)

2.5 N_2 adsorption-desorption isotherm

From Fig.11, it could be observed that the relative pressure P/P_0 between 0.4 and 1.0 appeared a hysteresis loop. According to the IUPAC classification, the isotherm of the CeO_2 crystals was attributed to the typical type Ⅳ isotherm[51]. Therefore, it could conclusive that CeO_2 crystals possessed mesoporous structure. The BET surface area, total pore volume and BJH pore diameter of the CeO_2 crystals were measured as 9 $m^2 \cdot g^{-1}$, 0.02 $cm^3 \cdot g^{-1}$ and 11.6 nm, respectively.

2.6 H_2-TPR

From Fig.12, it could be observed that the function of the H_2 consumption of CeO_2 crystals recorded in the range from 50~900 ℃. Two strong absorption peaks occurred at 516.7 and 771.9 ℃. According to the software corresponding to the

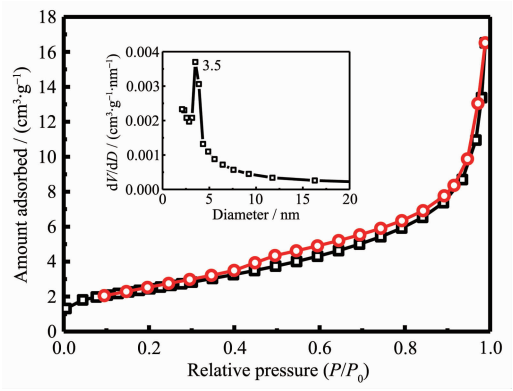

Inset: Corresponding BJH pore size distribution curves

Fig.11　N_2 adsorption-desorption isotherms of as-obtained flaky-like CeO_2 crystals

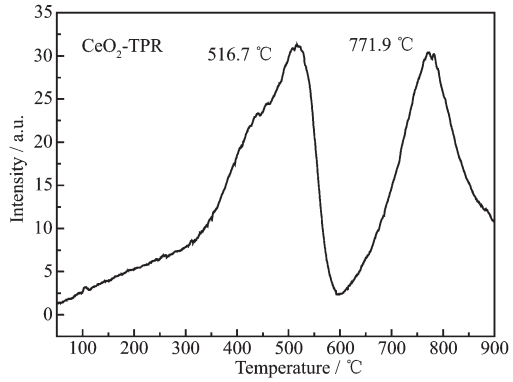

Fig.12　H_2-TPR profile of as-prepared flake-like CeO_2 crystals

TP5080 instrument, the amount of H_2 consumption of CeO_2 crystals could be calculated as 6.362 mmol·g^{-1}, indicating that the CeO_2 crystals had good reduction performance[52].

2.7　CO_2-TPD

From Fig.13, it could be observed that CO_2 consumption of CeO_2 crystals is a function of temperature in the range of 50~900 ℃. According to the software corresponding to the TP5080 instrument, the amount of CO_2 consumption of the CeO_2 crystals at different temperatures (room temperature, 120 and 700 ℃) could be calculated as 0.554, 0.527 and 0.059 mmol·g^{-1}, respectively. Adsorption capacity at room temperature was higher than previous reports (7.8, 11.6 mg·g^{-1})[52-53]. According to the analysis of the data, the capability of flake-like CeO_2 crystals to adsorb CO_2 was gradually weakening with the increase of adsorption temperature. This might be caused by an excessively high temperature resulting in the flake-like CeO_2 crystals being sintered and the basic sites losing their activity.

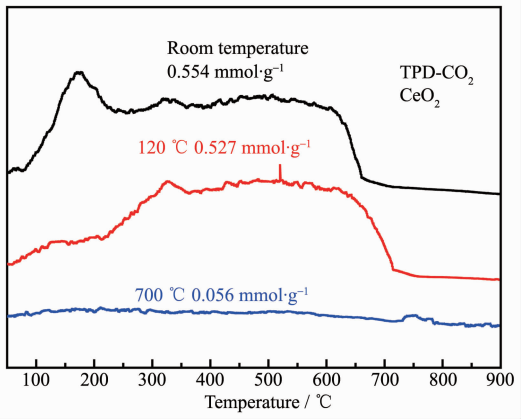

Fig.13　CO_2-TPR profile of as-prepared flake-like CeO_2 crystals

3　Conclusions

The flake-like CCPs were prepared by the stirring method, and the flake-like CeO_2 crystals were prepared by further calcining the flake-like CCPs at 500 ℃ for 4 h. The preparation conditions were finally confirmed as follows: 0.1 g CO_2SM with 50 mL 0.03 mol·L^{-1} Ce^{3+} aqueous solution, at room temperature and 1 000 r·min^{-1} for 0.5 h. The CO_2SM could not only provide CO_3^{2-} but also as a dispersant and structure directing agent. A large amount of the flake-like CCPs could be quickly prepared at room temperature. The flake-like CeO_2 crystals had good reduction performance and 0.554 mmol·g^{-1}, CO_2 adsorption at room temperature. This study not only proposed a new method for the synthesis of metal oxide, but also contributed to investigate the ability to adsorb CO_2.

Acknowledgments: This work was supported by Key Laboratory of Coal-based CO_2 Capture and Geological Storage (Jiangsu Province, China University of Mining and Technology, Grant No.2016A06), the National Natural Science Foundation of China (Grant No.21666027), the Program for Grassland Excellent Talents of Inner Mongolia Autonomous Region, the Natural Science Foundation of Inner Mongolia Autonomous Region (Grant No.2016JQ02) the Inner Mongolia Science and Technology Key Projects, and training plan of academic backbone in youth of Inner Mongolia University of Technology.

References:

[1] House K Z, Harvey C F, Azizc M J, et al. *Energy Environ. Sci.*, **2009**,**2**:193-205

[2] Abas N, Khan N. *J. CO_2 Util.*, **2014**,**8**:39-48

[3] Solomon S, Plattner G K, Knutti R, et al. *PNAS*, **2009**,**106**:1704-1709

[4] Chowdhury F A, Okabe H, Yamada H, et al. *Energy Procedia*, **2011**,**4**:201-208

[5] Rochelle G T. *Science*, **2009**,**325**:1652-1654

[6] Baltrusaitis J, Grassian V H. *J. Phys. Chem. B*, **2005**,**109**:12227-12230

[7] Baltrusaitis J, Schuttlefield J, Zeitler E, et al. *Chem. Eng. J.*, **2011**,**170**:471-481

[8] Li G, Xiao P, Webley P. *Langmuir*, **2009**,**25**:10666-10675

[9] Mosqueda H A, Vazquez C, Bosch P, et al. *Chem. Mater.*, **2006**,**18**:2307-2310

[10]Hornebecq V, Knofel C, Boulet P, et al. *J. Phys. Chem. C*, **2011**,**115**:10097-10103

[11]Carruthers J D, Petruska M A, Sturm E A, et al. *Microporous Mesoporous Mater.*, **2012**,**154**:62-67

[12]D′Alessandro D M, Smit B, Long J R. *Angew. Chem. Int. Ed.*, **2010**,**49**:6058-6082

[13]Samanta A, Zhao A, Shimizu G K H, et al. *Ind. Eng. Chem. Res.*, **2012**,**51**:1438-1463

[14]Chaikittisilp W, Khunsupat R, Chen T T, et al. *Ind. Eng. Chem. Res.*, **2011**,**50**:14203-14210

[15]Chaikittisilp W, Kim H, Jones C W. *Energy Fuels*, **2011**,**25**:5528-5537

[16]Yu J G, Le Y, Cheng B. *RSC Adv.*, **2012**,**2**:6784-6791

[17]Le Y, Guo D P, Cheng B, et al. *J. Colloid Interface Sci.*, **2013**,**408**:173-180

[18]Queen W L, Brown C M, Britt D K, et al. *J. Phys. Chem. C*, **2011**,**115**:24915-24919

[19]Sumida K, Rogow D L, Mason J A, et al. *Chem. Rev.*, **2012**,**112**:724-781

[20]Ren Y, Ma Z, Bruce P G. *Chem. Soc. Rev.*, **2012**,**41**:4909-4927

[21]Shang J, Li G, Singh R, et al. *J. Am. Chem. Soc.*, **2012**,**134**:19246-19253

[22]Lozinska M M, Mangano E, Mowat J P S. *J. Am. Chem. Soc.*, **2012**,**134**:17628-17642

[23]Pham T D, Liu Q, Lobo R F. *Langmuir*, **2013**,**29**:832-839

[24]Kamimura Y, Shimomura M, Endo A. *J. Colloid Interface Sci.*, **2014**,**436**:52-62

[25]Li C, Sakata Y, Arai T, et al. *J. Chem. Soc.*, **1989**,**85**:1451-1461

[26]Binet C, Daturi M, Lavalley J. *Catal. Today*, **1999**,**50**:207-225

[27]Zou Y L, Li Y, Zhang N, et al. *Adv. Mater. Res.*, **2012**,**557**:577-580

[28]Mai H X, Sun L D, Zhang Y W, et al. *J. Phys. Chem. B*, **2005**,**109**:24380-24385

[29]Laberty-Robert C, Long J W, Lucas E M, et al. *Chem. Mater.*, **2006**,**18**:50-58

[30]Murai S, Fujita K, Iwata K, et al. *J. Phys. Chem. C*, **2011**,**115**:17676-17681

[31]Yao H B, Wang Y J, Luo G S. *Ind. Eng. Chem. Res.*, **2017**,**56**:4993-4999

[32]Zhang D S, Niu F H, Li H R, et al. *Powder Technol.*, **2011**,**207**:35-41

[33]Devaraju M K, Yin S, Sato T. *ACS Appl. Mater. Interfaces*, **2009**,**11**:2694-2698

[34]Riccardi C S, Lima R C, Santos M L, et al. *Solid State Ionics*, **2009**,**180**:288-291

[35]Cao C Y, Cui Z M, Chen C Q, et al. *J. Phys. Chem. C*, **2010**,**114**:9865-9870

[36]Duan P Q, Huang T T, Xiong W, et al. *Langmuir*, **2017**,**33**:2454-2459

[37]Min B H, Lee J C, Jung K Y, et al. *RSC Adv.*, **2016**,**6**:81203-81210

[38]Yoshikawa K, Kaneeda M, Nakamura H. *Energy Procedia*, **2017**,**114**:2481-2487

[39]Zhao T X, Guo B, Han L M, et al. *ChemPhysChem*, **2015**,**16**:2106-2109

[40]Zhai Y Q, Zhang S Y, Pang H. *Mater. Lett.*, **2007**,**61**:1863-1866

[41]Shang X F, Lu W C, Yue B H, et al. *Cryst. Growth Des.*, **2009**,**9**:1415-1420

[42]Wang S F, Gu F, Li C Z, et al. *J. Cryst. Growth*, **2007**,**307**:386-394

[43]Yang W, Jiang Z H, Yang J, et al. *Ind. Eng. Chem. Res.*, **2015**,**54**:11048-11055

[44]Jeevanandam P, Koltypin Y, Palchik O, et al. *J. Mater. Chem.*, **2001**,**11**:869-873

[45]Dai Q G, Bai S X, Li H, et al. *CrystEngComm*, **2014**,**16**:9817-9827

[46]Jiang J X, Ye J Z, Zhang G W, et al. *J. Am. Ceram. Soc.*, **2012**,**95**:3735-3738

[47]Caswell K K, Bender C M, Murphy C J. *Nano Lett.*, **2003**,**3**:667-669

[48]Xu X Y, Zhao Y, Lai Q Y, et al. *J. Appl. Polym. Sci.*, **2011**,**119**:319-324

[49]Zhang J C, Yang H X, Wang S P, et al. *CrystEngComm*, **2014**,**16**:8777-8785

[50]Liu W, Deng T, Feng L J, et al. *CrystEngComm*, **2015**,**17**:4850-4858

[51]Zhou H P, Zhang Y W, Si R, et al. *J. Phys. Chem. C*, **2008**,**112**:20366-20374

[52]Li C C, Liu X H, Lu G Z, et al. *Chin. J. Catal.*, **2014**,**35**:1364-1375

[53]Wang Y G, Yin C C, Qin H F. *Dalton Trans.*, **2015**,**44**:18718-18722